C^∞ Smooth Freeform Surfaces Over Hyperbolic Domains

Wei Zeng
Stony Brook University
zengwei@cs.sunysb.edu

Ying He Jiazhi Xia
Nanyang Technological University
{yhe|xiaj0002}@ntu.edu.sg

Xianfeng Gu Hong Qin
Stony Brook University
{gu|qin}@cs.sunysb.edu

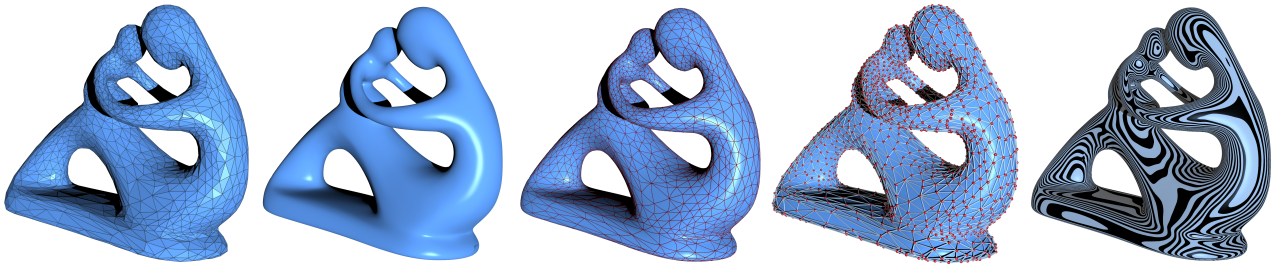

(a) (b) (c) (d) (e)

Figure 1: *Modeling real-world shapes using hyperbolic freeform surface. (a) The input is a triangular mesh of genus 4. (b) Our approach generates a C^∞ smooth surface using hyperbolic structure. The red curves in (c) show the images of the triangulation. (d) shows the control points overlaid with the smooth surface. The isophotes in (f) demonstrate the high quality of the constructed surface.*

Abstract

Constructing smooth freeform surfaces of arbitrary topology with higher order continuity is one of the most fundamental problems in shape and solid modeling. Most real-world surfaces are with negative Euler characteristic number $\chi = 2 - 2g - b < 0$, where g is genus, b is the number of boundaries. This paper articulates a novel method to construct C^∞ smooth surfaces with negative Euler numbers based on hyperbolic geometry and discrete curvature flow. According to Riemann uniformization theorem, every surface with negative Euler number has a unique conformal Riemannian metric, which induces Gaussian curvature of -1 everywhere. Hence, the surface admits hyperbolic geometry. Such uniformization metric can be computed using the discrete curvature flow method: hyperbolic Ricci flow. Consequently, the basis function for each control point can be naturally defined over a hyperbolic disk, and through the use of partition-of-unity, we build a freeform surface directly over hyperbolic domains while having C^∞ property. The use of radial, exponential basis functions gives rise to a true meshless method for modeling freeform surfaces with greatest flexibilities, without worrying about control point connectivity. Our algorithm is general for arbitrary surfaces with negative Euler characteristic. Furthermore, it is C^∞ continuous everywhere across the entire hyperbolic domain without singularities. Our experimental results demonstrate the efficiency and efficacy of the proposed new approach for shape and solid modeling.

CR Categories: I.3.5 [Computing Methodologies]: Computer Graphics—Computational Geometry and Object Modeling; G.2.1 [Mathematics of Computing]: Discrete Mathematics—Combinatorics

Keywords: Manifold, Hyperbolic Structure, Universal Covering Space, Curvature Flow, Uniformization Metric

1 Introduction and Motivation

Real-world objects are oftentimes of complex structure and arbitrary topology. One fundamental goal of solid and physical modeling is to seek accurate and effective techniques for the compact representation of smooth freeform shapes with higher-order continuity and without any singularity (that would require special care otherwise). To date, tremendous efforts have been devoted for constructing freeform splines on surfaces with complicated topologies by generalizing conventional spline schemes from Euclidean domains to arbitrary manifolds. In a recently-developed manifold spline framework, [Gu et al. 2006] pointed out that conventional spline schemes are based on polar forms [Seidel 1993] that are parametric affine invariant. Therefore, defining manifold splines based on polar form is equivalent to defining affine geometry on the surface. Unfortunately, due to the topological obstruction, surfaces with non-zero Euler number do not admit affine geometry. The recent result by Gu et al. showed that the number of extraordinary points of manifold splines with genus $g > 1$ can be reduced to as small as one [Gu et al. 2008]. This is the intrinsic reason why the conventional polynomial-based approach cannot achieve global continuity, while the singularity point cannot be completely avoided.

Due to the existence of extraordinary points in polynomial-based manifold splines, the current state of the art is far from adequate mainly because of the two following aspects. First, the existence of extraordinary points requires a great deal of special care such as hole filling from users (e.g., filling the holes using a separate spline surface [Gu et al. 2008], or using recursive subdivision to shrink the size of the vicinity of hole regions [Wang et al. 2009], or other strategies). All of these delicate strategies require tremendous amount of human intervention and labor. Second, higher-order continuity cannot be easily satisfied without explicitly increasing the degree of the underlying polynomial basis functions, as a result, polynomials must be degree-elevated in order to satisfy continuity-varying (in both spatial and temporal domains) design and modeling requirements, which is not flexible and far from ideal.

From the practical and algorithmic standpoint, it is highly desirable to construct smooth surfaces without singularities. Thus, one feasible way is to get rid of the polynomial or rational polynomial requirements and directly use non-polynomial smooth functions, such as exponential functions, to define the shape geometry. Grimm and Hughes [1995] pioneered a method to construct C^k-continuous parametric surfaces over triangle and quadrilateral meshes. Following this direction, there has been extensive research for manifold construction [Navau and Garcia 2000; Ying and Zorin 2004; Gal-

lier et al. 2009; Vecchia et al. 2008; Siqueira et al. 2009].

In this paper, we present a new method to construct smooth freeform surfaces with negative Euler characteristic number, $\chi = 2 - 2g - b < 0$, where g is genus, b is the number of boundaries. Most real-world surfaces are of genus $g > 1$, i.e. with negative Euler number. Here, we focus on high genus surfaces. Surfaces with boundaries can be converted to closed surfaces by double covering [Gu and Yau 2003]. The constructed surfaces can be defined on arbitrary triangular meshes with $\chi < 0$ and are C^∞ continuous everywhere. Our approach is based on the following observation that the Riemannian metric of these surfaces can be conformally deformed by Ricci flow such that the Gaussian curvatures eventually become constant -1 everywhere, namely, the final Riemannian metric is hyperbolic. Therefore, hyperbolic geometry can be potentially utilized for defining basis functions. More specifically, in order to effectively compute all basis functions, we use Poincaré disk as the underlying domain for 2 dimensional hyperbolic space $\mathbb{H}^2$. Given a surface $(S, \mathbf{g})$ with a hyperbolic metric $\mathbf{g}$, we can compute an open covering of the surface $\{U_\alpha\}$, $S \subset \bigcup_\alpha U_\alpha$. Then we map each open set U_α onto the Poincaré disk, $\phi_\alpha : U_\alpha \to \mathbb{H}^2$. The atlas $A = \{(U_\alpha, \phi_\alpha)\}$ gives a hyperbolic structure [Jin et al. 2008], the local parameter transitions

$$\phi_{\alpha\beta} = \phi_\beta \circ \phi_\alpha^{-1} : \phi_\alpha(U_\alpha \bigcap U_\beta) \to \phi_\beta(U_\alpha \bigcap U_\beta)$$

must be rigid motions in the hyperbolic space. All the hyperbolic geometric quantities can be directly measured on the hyperbolic parameter domain, and the measurement is independent of the choice of the chart. Therefore, hyperbolic geometry is well defined on the surface via the hyperbolic structure. In addition, this naturally paves the new way for us to define scalar functions directly over hyperbolic geometry. Because of many intrinsic properties (both theoretical and computational) associated with hyperbolic geometry structure, it is both natural and necessary to define vector-valued functions and use control points to blend with these functions over hyperbolic geometry. As a result, parameterization-centered freeform surfaces can be naturally defined, manipulated for surface modeling and representation. Figure 1 shows an example of modeling real-world shapes using hyperbolic freeform surface. Our method has the following advantages:

- It is **general** for arbitrary surfaces with negative Euler characteristic and **independent of combinatorial structure** (i.e. triangulation).
- The constructed surface has the property of C^∞ **continuity** and **without any singularity** in the setting of the hyperbolic uniformization metric.

2 Previous Work

There are some related work on defining singularity-free functions on manifold. Grimm and Hughes constructed an atlas of an arbitrary mesh in [1995], where the chart transition functions are rotation, translation, projective and spline blending functions. Navau and Garcia [2000] introduced another method to construct manifold based on subdivision surface, the chart transitions are either affine or polynomial. The construction of the atlas depends on the combinatorial structure of the mesh. Ying and Zorin [2004] used analytic functions as chart transition to build an analytic atlas. The construction is also determined by the mesh structure. Parametric pseudo-manifolds (PPM's) have been used for smooth surface construction from polygonal meshes in [Gallier et al. 2009] and [Siqueira et al. 2009], where the atlas construction is also determined by the mesh structure. Rational blending manifold is constructed in [Vecchia et al. 2008], where all the chart transitions are rational functions.

These methods share similar construction procedures which can be summarized as follows:

1. Find an atlas $\{U_i, \phi_i\}$ to cover the domain manifold M, with transition functions $\phi_{ij} = \phi_j \circ \phi_i^{-1}$. All transition functions are required to be smooth.
2. Define functional basis on each chart $f_i : \phi_i(U_i) \to R$.
3. For each point $p \in M$, normalize these functions and define the basis functions B_i as

$$B_i(p) = \frac{f_i(p)}{\sum_j f_j(p)}.$$

4. Define the functions as $F(p) = \sum_i C_i B_i(p)$ where C_i are the control points.

Our method follows the same framework but different in that

1. All the above methods construct atlas based on the mesh structure. In contrast, the atlas in our method is solely determined by the geometry of the surface, more rigorously, the conformal structure of the surface. In theory, it is independent of the triangulation. Therefore our method is more intrinsic.
2. Our free-form surface is constructed by using hyperbolic geometry, this requires that all the chart transitions are hyperbolic rigid motions. Namely, we define hyperbolic geometry on general surfaces. Most of the above approaches use smooth functions for the transition functions. There is no associated geometry defined on the surface.

   Furthermore, the local parameters in our atlas are conformal to the original surface, therefore the atlas is determined by the conformal structure of the surface. The transitions of the atlas in [Ying and Zorin 2004] are also analytical functions, but it is solely determined by the combinatorial structure of the mesh, and irrelevant to the conformal structure of the original surface.
3. The functional basis f_i is an exponential function defined on hyperbolic disk. The existing approaches define the functional basis on either $\mathbb{R}^2$ or $\mathbb{C}^2$.

Note that both the transition functions and functional basis of our approach are C^∞-continuous, thus, the resulting surface is C^∞ continuity everywhere. Furthermore, our approach applies to triangular meshes with arbitrary triangulation.

3 Theoretic Background

This section briefly introduces the theoretic background necessary for the current work. For details, we refer readers to [R.Munkres 1984] for algebraic topology, [Schoen and Yau 1994] for differential geometry and [Jin et al. 2008] for Ricci flow.

3.1 Fundamental group and representative of homotopy class

Let S be a topological surface, and let p be a point of S. All loops with base point p are classified by homotopy relation. All homotopy equivalence classes form the *homotopy group* or *fundamental group* $\pi_1(S, p)$, where the product is defined as the concatenation of two loops through their common base point.

Suppose S is a genus g closed surface. A *canonical set of generators* of $\pi(S, p)$ consists of $\{a_1, b_1, a_2, b_2, \cdots, a_g, b_g\}$, such

that the pair a_i and b_i has one intersection point, the pairs $\{a_i, a_j\}$, $\{b_i, b_j\}$ and $\{a_i, b_j\}$, have no intersections, where $i \neq j$. See Figure 2 for an example of canonical basis on a genus two surface.

3.2 Universal cover

A *covering space* of S is a space $\tilde{S}$ together with a continuous surjective map $h : \tilde{S} \to S$, such that for every $p \in S$ there exists an open neighborhood U of p such that $h^{-1}(U)$ (the inverse image of U under h) is a disjoint union of open sets in $\tilde{S}$ each of which is mapped homeomorphically onto U by h. The map h is called the *covering map*. A simply connected covering space is a *universal cover*.

A *deck transformation* of a cover $h : \tilde{S} \to S$ is a homeomorphism $f : \tilde{S} \to \tilde{S}$ such that $h \circ f = h$. All deck transformations form a group, the so-called *deck transformation group*. A *fundamental domain* of S is a simply connected domain, which intersects each orbit of the deck transformation group only once.

3.3 Uniformization metric

Let S be a surface embedded in $\mathbb{R}^3$. S has a Riemannian metric induced from the Euclidean metric of $\mathbb{R}^3$, denoted by $\mathbf{g}$. Suppose $u : S \to \mathbb{R}$ is a scalar function defined on S. Then $\bar{\mathbf{g}} = e^{2u}\mathbf{g}$ is also a Riemannian metric on S and is conformal to the original one.

The *uniformization theorem* for surfaces says that any metric surface admits a Riemannian metric of constant Gaussian curvature, which is conformal to the original metric. Such metric is called the *uniformization metric*.

For surface with negative Euler characteristic, the Gaussian curvature is -1 under uniformization metric. Uniformization metric can be solved using Ricci flow, where the Gaussian curvatures are deformed by the following PDE:

$$\bar{K} = e^{-2u}(-\Delta_{\mathbf{g}} u + K),$$

where $\Delta_{\mathbf{g}}$ is the Laplacian-Beltrami operator under the original metric $\mathbf{g}$. The above equation is called the *Yamabe equation*. By solving the Yamabe equation, one can design a conformal metric $e^{2u}\mathbf{g}$ by a prescribed curvature $\bar{K}$.

3.4 Poincaré disk model

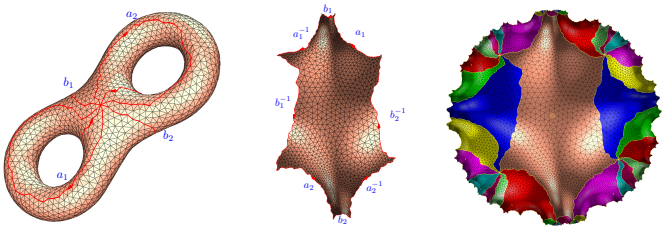

(a) homotopy group (b) fundamental domain (c) portion of UCS

Figure 2: *Computing the hyperbolic structure of genus-2 model. (a) Compute a set of canonical fundamental group basis $\{a_1, b_1, a_2, b_2\}$; (b) Compute the hyperbolic uniformization metric using hyperbolic Ricci flow. The fundamental domain is isometrically embedded onto $\mathbb{H}^2$ under the hyperbolic metric; (c) Compute the Fuchsian group generators. Any finite portion of the universal covering space (UCS) can be constructed using these generators.*

In this work, we use Poincaré disk to model the hyperbolic space $\mathbb{H}^2$, which is the unit disk $|z| < 1$ on the complex plane with the metric

$$ds^2 = \frac{4dzd\bar{z}}{(1 - z\bar{z})^2}.$$

The rigid motion is the Möbius transformation

$$z \to e^{i\theta}\frac{z - z_0}{1 - \bar{z}_0 z},$$

where θ and z_0 are parameters. The geodesic of Poincaré disk is a Euclidean circular arc, which is perpendicular to the unit circle as shown in Figure 3 (a).

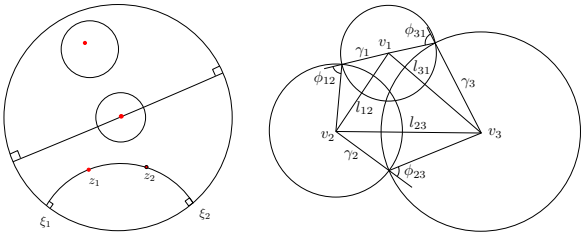

(a) (b)

Figure 3: *(a) Hyperbolic line and circles on Poincaré disk. (b) Circle packing metric.*

Suppose S is a high genus closed surface with the hyperbolic uniformization metric $\tilde{\mathbf{g}}$. Then its universal covering space $(\tilde{S}, \tilde{\mathbf{g}})$ can be isometrically embedded in $\mathbb{H}^2$. Any deck transformation of $\tilde{S}$ is a Möbius transformation, and called a *Fuchsian transformation*. The deck transformation group is called the *Fuchsian group* of S.

The geodesics, or hyperbolic lines, are circular arcs perpendicular to the unit circle. Let z_1 and z_2 be two points inside the Poincaré disk, then there exits a unique geodesic passing through z_1 and z_2. Suppose the geodesic intersects the unit circle at ξ_1, ξ_2, ξ_1 is closer to z_1 and ξ_2 is closer to z_2, then hyperbolic distance between z_1, z_2 is given by

$$\log[z_1, z_2; \xi_1, \xi_2]^{-1},$$

where the complex cross ratio

$$[z_1, z_2; \xi_1, \xi_2] = \frac{(z_1 - \xi_1)(z_2 - \xi_2)}{(z_2 - \xi_1)(z_1 - \xi_2)}$$

is a real number, because four points z_1, z_2, ξ_1, ξ_2 are on the same circle.

A hyperbolic circles (c, r) on the Poincaré disk, where c is the center, r is the radius, is a Euclidean circles (C, R), where

$$C = \frac{2 - 2\mu^2}{1 - \mu^2|c|^2}c, R^2 = |C|^2 - \frac{|c|^2 - \mu^2}{1 - \mu^2|c|^2},$$

where $\mu = 2\cosh(r)$.

3.5 Discrete Hyperbolic Ricci Flow

In practice, all surfaces are approximated by triangular meshes. Let M be a triangular mesh, $\{v_1, v_2, \cdots, v_n\}$ be the vertex set, $[v_i, v_j]$ be an edge connecting v_i and v_j, $[v_i, v_j, v_k]$ be a face. Then the *discrete metric* of M is the edge lengths. Let θ_i^{jk} be the corner angle at vertex v_i in the face $[v_i, v_j, v_k]$. We treat each face $[v_i, v_j, v_k]$ as a hyperbolic triangle, therefore θ_i^{jk} is determined by the edge lengths using hyperbolic cosine law. The *discrete Gaussian curvature* is defined as the angle deficit,

$$K_i = \begin{cases} 2\pi - \sum \theta_i^{jk} & v_i \notin \partial M \\ \pi - \sum \theta_i^{jk} & v_i \in \partial M \end{cases}.$$

We define circle packing metric on M in the following way. Let M be a triangular mesh. We associate each vertex v_i with a disk with radius γ_i. On edge $e_{ij} = [v_i, v_j]$, the two circles intersect at the angle ϕ_{ij}. Then the edge length $l_{ij}$of e_{ij} is determined by the hyperbolic cosine law:

$$\cosh l_{ij} = \cosh \gamma_i \cosh \gamma_j + \sinh \gamma_i \sinh \gamma_j \cos \phi_{ij}. \quad (1)$$

A *circle packing metric* is denoted as (M, Γ, Φ), where $\Gamma : v_i \to \gamma_i$ represents the radius, $\Phi : e_{ij} \to \phi_{ij}$ represents the intersection angle. See Figure 3 (b).

Let $u_i = \log \tanh \frac{\gamma_i}{2}$, $\mathbf{u} = (u_1, u_2, \cdots, u_n)$, then *the discrete Ricci flow* is defined as

$$\frac{du_i(t)}{dt} = -K_i, \quad (2)$$

where K_i is the discrete Gaussian curvature at v_i. The convergence of the discrete hyperbolic Ricci flow is proven by Chow and Luo [Chow and F.Luo 2003].

The *Ricci energy* for circle packing metric (M, Γ, Φ) is defined as

$$E(\mathbf{u}) = \int_{\mathbf{u}_0}^{\mathbf{u}} \sum_{i=1}^{n} (\bar{K}_i - K_i) du_i, \quad (3)$$

where $\mathbf{u}_0 = (0, 0, \cdots, 0)$.

The discrete hyperbolic Ricci energy is convex. It has a unique global minimum, which induces the target curvature $\bar{K}_i$. Therefore, in order to compute the uniformization metric, we can set the target curvature $\bar{K}_i \equiv 0$ for all vertices, and optimize the Ricci energy using Newton's method.

4 Construction of C^∞-Continuous Surfaces

The basic idea of this work is straight forward. Most surfaces with complicated topologies are with negative Euler characteristic. Although they do not admit affine geometry, they do admit hyperbolic geometry. Given a triangular mesh M with negative Euler characteristic, M serves both the domain manifold and control net. Our construction has the following two steps:

1. **Computing the hyperbolic structure of** M We compute the uniformization metric using discrete Ricci flow and isometrically embed the mesh onto the hyperbolic disk using Poincaré model. This constructs hyperbolic atlas, such that all local coordinate transitions are hyperbolic rigid transformations, i.e., Möbius transformation.

2. **Defining the basis function** We associate a basis function for each control point $\mathbf{c}_i \in M$. The basis function is a C^∞-continuous function defined on a hyperbolic disk $D(\mathbf{c}_i, r_i) \in M$, centered at $\mathbf{c}_i$ and with radius r_i, and thus, has finite support. Given a point $p \in M$ on the domain manifold M, the evaluation at p can be carried out by finding all control points whose supporting functions cover p, and then take the weighted sum of their basis functions.

4.1 Computing the hyperbolic structure

We compute the hyperbolic uniformization metric using hyperbolic Ricci flow, compute the fundamental group generators and the corresponding Fuchsian group generators. Figure 2 illustrates the pipeline. Suppose we are given a mesh with negative Euler number, as shown in frame (a).

1. Use hyperbolic Ricci flow introduced in the previous section to compute the hyperbolic metric, such that all vertex curvature equals to zero.

2. Compute a set of canonical fundamental group generators through a base vertex, as shown in frame (b). We use the method from Ericson [Erickson and Whittlesey 2005]. We denote the generators as $\{a_1, b_1, a_2, b_2, \cdots, a_g, b_g\}$.

3. Slice the mesh M along the fundamental group generators to get an open mesh $\bar{M}$. The boundary of $\bar{M}$ is

$$\partial \bar{M} = a_1 b_1 a_1^{-1} b_1^{-1} \cdots a_g b_g a_g^{-1} b_g^{-1}.$$

   Isometrically embed $\bar{M}$ onto the Poincaré disk using the hyperbolic uniformization metric to get a fundamental domain, still denoted as $\bar{M}$. As shown in frame (c). The embedding method is similar to that in [Jin et al. 2008].

4. Compute the Fuchsian group generators corresponding to the fundamental group generators. Let γ be a fundamental group generator. Because $\bar{M}$ has been embedded onto the Poincaré disk, $\gamma \in \partial \bar{M}$, we treat γ as a curve segment on the Poincaré disk. We compute the unique Fuchsian transformation ϕ, such that ϕ maps γ^{-1} to γ. First a Möbius transformation can be calculated such that the starting vertex of γ is mapped to the origin, the ending vertex is mapped to a positive real number. Similarly we find another Möbius transformation for γ^{-1}. The composition of the second map with the inverse of the first map is the desired Fuchsian transformation. We denote the Fuchsian transformations as α_i corresponding to a_i, β_j corresponding to b_j.

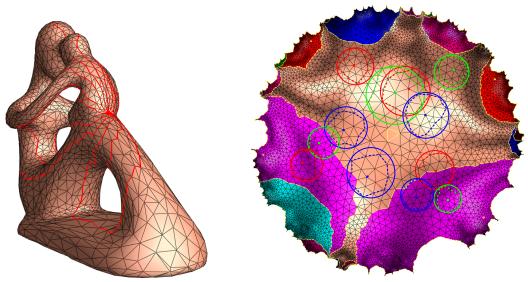

Figure 4: *Hyperbolic structures of the genus-4 fertility model. The colored circles show the support of base functions. Note that, hyperbolic circles on Poincaré disk looks like Euclidean circles, but the centers do not coincide with the Euclidean circle centers. The control points are at the centers of the hyperbolic circles. The dotted poly-lines show the two ring neighbor of the control points.*

Figure 4 demonstrates the hyperbolic atlas of a genus-4 surface.

4.2 Defining the functional basis

We define the geometry of the constructed surface using hyperbolic partition of unity. Let $(M, \mathbf{g})$ be the surface with a hyperbolic Riemannian metric $\mathbf{g}$ which is computed by hyperbolic Ricci flow. A hyperbolic disk $D(c, r) \subset M$ be an open hyperbolic disk on M, with center $c \in M$ and radius $r > 0$,

$$D(c, r) := \{p \in M | d_{\mathbf{g}}(c, p) < r\}$$

where $d_{\mathbf{g}}(c, p)$ measures the hyperbolic distance between c and p on M under metric $\mathbf{g}$. The *radial function* $f_D : D(c, r) \to \mathbb{R}^+$ is defined as follows,

$$f_D(p) = \begin{cases} C \exp(\frac{-1}{(d_{\mathbf{g}}(c,p)-r)^2}) & p \in D(c, r) \\ 0 & p \notin D(c, r) \end{cases}$$

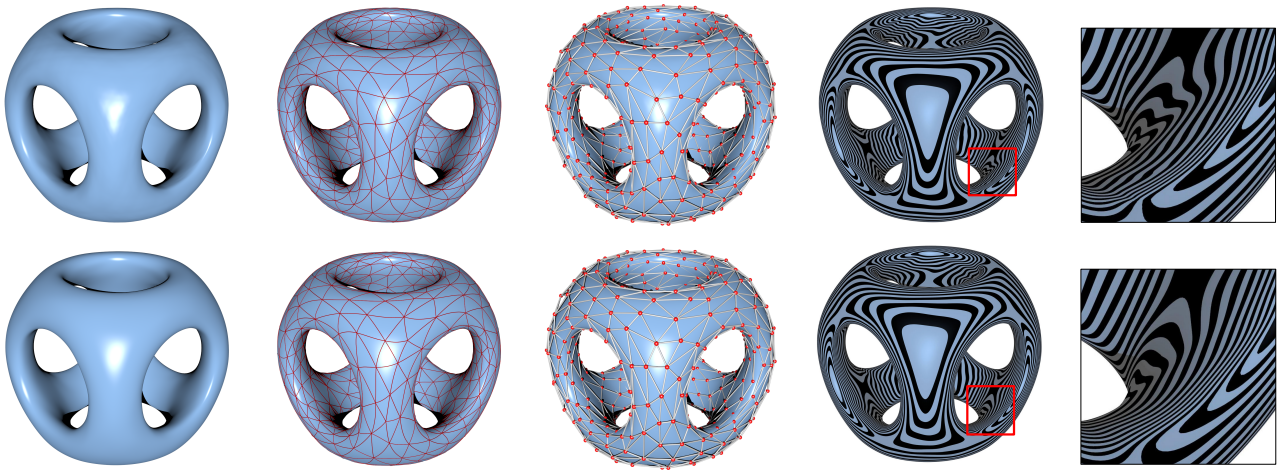

(a) (b) (c) (d) (e)

Figure 5: *Comparison to Loop subdivision. Loop subdivision is C^2 continuous except at the extraordinary points which has only C^1 continuity. Our approach is C^∞ continuous everywhere. Although these two surfaces look similar (see (a)) and even have similar triangulation (see (b-c)), the isophotes in (d) and the close-up view in (e) reveal the difference of the surface quality. To make the comparison fair, the hyperbolic function is evaluated at the same resolution as the Loop subdivision which the 4-th level subdivision is employed.*

where $C = \exp(\frac{1}{r^2})$. Then f_D has the following properties:

- f_D is infinitely smooth, $f_D \in C^\infty(D, \mathbb{R})$;
- f_D has finite support, $supp(f_D) = D$;
- f_D is non-negative and $f_D(c)$ equals to one.

Let $\{\mathbf{c_i}\}$ be the set of all control points, i.e., the vertex of the input mesh M. We associate each control point $\mathbf{c}_i$ with a hyperbolic disk $D_i \in M$ with radius r_i such that D_i is the smallest hyperbolic disk to cover $\mathbf{c}_i$ and its two-ring neighbors under hyperbolic metric $\mathbf{g}$, as shown in Figure 4. Let $\{D_\alpha\}$ be a collection of open hyperbolic disks on M, such that
1. The union of D_α's covers the surface, $M \subset \bigcup_\alpha D_\alpha$.
2. Each point on the surface is covered by finite number of disks. Namely $\forall p \in M$, there is finite number of open sets D_α, such that $p \in D_\alpha$.

Then the hyperbolic freeform surface (HFS) $F : M \to \mathbb{R}^3$ is defined as

$$F(p) = \sum_i \mathbf{c_i} f_i(p),$$

where $f_i(p) = f_{D_i}(p) / \sum_j f_{D_j}(p)$ and D_j is a hyperbolic disk covering the point p, i.e., $p \in D_j$. The evaluation of the hyperbolic freeform surface $F(p)$ can be carried out by finding all control points whose supporting function (the hyperbolic disc) covers the point p. Because of the properties of the hyperbolic partition of unity, the constructed surface has the following properties:

- Infinite global smoothness since the transition functions and basis functions are C^∞ continuous.
- No extraordinary points since the surface admits a hyperbolic atlas.
- Affine invariant. If an affine transformation is applied to the surface, the result can be constructed from the affine images of its control points.

5 Experimental Results

We tested our prototype system on a workstation with a 2.66GHz CPU and 3GB memory. Table 1 summarizes our experimental results. The times for computing hyperbolic metric and for embedding the one-ring neighborhood of the central fundamental domain are reported. It can be easily seen that the hyperbolic metric computation is proportional to the number of faces and independent of genus; whereas the time for hyperbolic embedding depends heavily on the number of genus. Constructing the functional basis is very efficient.

Figure 5 shows the comparison of our approach to Loop subdivision [Loop 1987]. Note that Loop subdivision surface is C^2-continuous except at the extraordinary points (vertex with valence other than 6) which are only C^1-continuous. Compared to Loop subdivision surfaces, the smoothness of our approach does not vary with the valence of the control mesh triangulation, and the constructed surface is C^∞-continuous everywhere. Figures 6 and 7 show the examples of constructed surfaces of various topological type. To demonstrate the proposed approach in shape modeling, we applied freeform deformation to the control nets and the deformed surfaces are still of C^∞ continuity everywhere as shown in Figure 8. The results prove both the theoretic rigor and feasibility in practice.

Table 1: *Statistics. N_c, # of control points; N_f, # of faces; g, genus; T_h, time of computing hyperbolic metric; T_e, time of one-ring embedding.*

Models	Figure	N_c	N_f	g	$T_h(s)$	$T_e(s)$
Fertility	Fig.1	2108	4228	4	22	20
Decocube1	Fig.5	492	1000	5	5	101
Decocube2	Fig.6	1234	2516	13	12	138
3-hole torus	Fig.6	746	1500	3	7	4
Pegaso	Fig.7	7990	16000	6	78	178
Kids	Fig.7	5986	12000	8	56	243

6 Conclusion

This paper has presented a new method to construct smooth surfaces with negative Euler characteristic. The constructed surfaces can be defined on arbitrary triangular meshes of $g > 1$ and are C^∞ continuous everywhere. The fundamentally new idea of our method is to find the hyperbolic atlas of the given mesh where the transition function is a hyperbolic rigid motion, i.e., Möbius transformation. Then hyperbolic partition of unity is applied to define

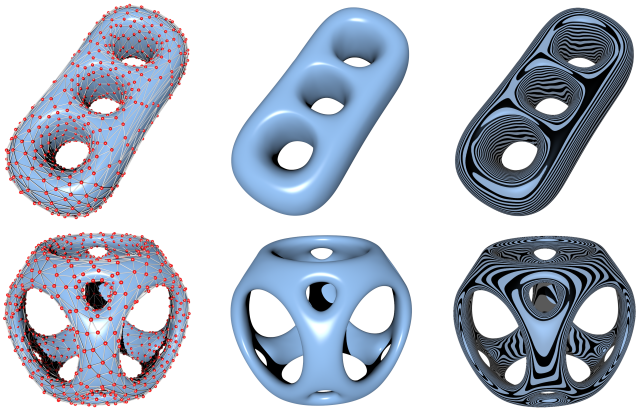

(a) control net (b) HFS (c) isophote

Figure 6: *Modeling synthetic shapes using hyperbolic freeform surface (HFS).*

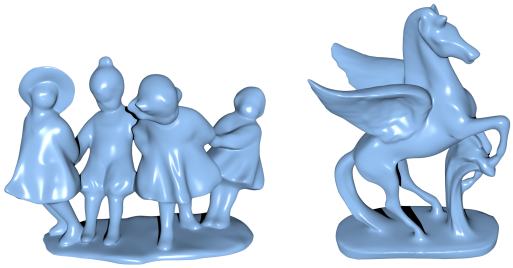

(a) Kids (b) Pegaso

Figure 7: *Modeling real-world shapes using hyperbolic freeform surface.*

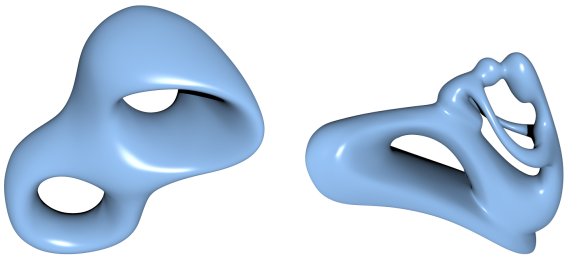

Figure 8: *Editing the shape by deforming the control points. The deformed surface is still C^∞-continuous everywhere.*

smooth freeform functional basis with finite support. Our approach can be applied to triangular mesh with arbitrary triangulation. Our experimental results demonstrate the efficiency and efficacy of the proposed approach in shape modeling.

Acknowledgments

Ying He and Jiazhi Xia are supported by the Singapore National Research Foundation Interactive Digital Media R&D Program, under research Grant NRF2008IDM-IDM004-006.

References

CHOW, B., AND F.LUO. 2003. Combinatorial ricci flows on surfaces. *Journal of Differential Geometry 63*, 1, 97–129.

ERICKSON, J., AND WHITTLESEY, K. 2005. Greedy optimal homotopy and homology generators. In *SODA*, Society for Industrial and Applied Mathematics, 1038–1046.

GALLIER, J., MORERA, D., NONATO, L., SIQUEIRA, M., VELHO, L., AND XU, D. 2009. Fittng surfaces to polygonal meshes using parametric pseudo-manifolds. In *XXI Brazilian Symposium on Computer Graphics and Image Processing*.

GRIMM, C., AND HUGHES, J. F. 1995. Modeling surfaces of arbitrary topology using manifolds. In *SIGGRAPH*, 359–368.

GU, X., AND YAU, S.-T. 2003. Global conformal parameterization. In *Symposium on Geometry Processing*, 127–137.

GU, X., HE, Y., AND QIN, H. 2006. Manifold splines. *Graphical Models 68*, 3, 237–254.

GU, X., HE, Y., JIN, M., LUO, F., QIN, H., AND YAU, S.-T. 2008. Manifold splines with a single extraordinary point. *Computer-Aided Design 40*, 6, 676–690.

JIN, M., KIM, J., LUO, F., AND GU, X. 2008. Discrete surface ricci flow. *IEEE TVCG 14*, 5, 1030–1043.

LOOP, C. 1987. *Smooth Subdivision Surfaces Based on Triangles*. Mathematics, University of Utah.

NAVAU, J. C., AND GARCIA, N. P. 2000. Modeling surfaces from meshes of arbitrary topology. *CAGD 17*, 7, 643–671.

R.MUNKRES, J. 1984. *Elements of Algebraic Topology*. Addison-Wesley Co.

SCHOEN, R., AND YAU, S.-T. 1994. *Lectures on Differential Geometry*. International Press of Boston.

SEIDEL, H.-P. 1993. An introduction to polar forms. *IEEE Comput. Graph. Appl. 13*, 1, 38–46.

SIQUEIRA, M., XU, D., GALLIER, J., NONATO, L., MORERA, D., AND VELHO, L. 2009. A new construction of smooth surfaces from triangle meshes using parametric pseudo-manifolds. *Computer & Graphics*.

VECCHIA, G. D., JÜTTLER, B., AND KIM, M.-S. 2008. A construction of rational manifold surfaces of arbitrary topology and smoothness from triangular meshes. *Computer Aided Geometric Design 25*, 9, 801–815.

WANG, H., HE, Y., LI, X., GU, X., AND QIN, H. 2009. Geometry-aware domain decomposition for T-spline-based manifold modeling. *Computer & Graphics 33*, 3, 359–368.

YING, L., AND ZORIN, D. 2004. A simple manifold-based construction of surfaces of arbitrary smoothness. *ACM Trans. Graph. 23*, 3, 271–275.

A Proof for C^∞ smoothness

Suppose S is a surface with negative Euler number. Then the hyperbolic freeform surface $F : S \to \mathbb{R}^3$ is with C^∞ smoothness.

Proof: The surface S is covered by a hyperbolic atlas. All local chart transitions are Möbius transformations. Möbius transformations are C^∞ continuous. Therefore, the surface S has a C^∞ differential structure.

In order to show $F : S \to \mathbb{R}^3$ is C^∞ continuous, it is sufficient and necessary to show it is C^∞ on one chart. In the following discussion, we focus on the behavior of F on one chart only.

The complex cross ratio

$$[z_1, z_2; \xi_1, \xi_2] = \frac{(z_1 - \xi_1)(z_2 - \xi_2)}{(z_2 - \xi_1)(z_1 - \xi_2)},$$

is C^∞ with respect to z_1 or z_2. Therefore, the hyperbolic distance

$$d(z_1, z_2) = \log[z_1, z_2; \xi_1, \xi_2]^{-1}$$

is C^∞ with respect to z_1 or z_2. As a result, the exponential function defined on the hyperbolic disc $f_D : D(c, r) \to \mathbb{R}$ is also C^∞ with respect to $d(c, p)$,

$$f_D(p) = \begin{cases} C \exp(\frac{-1}{(d(c,p)-r)^2}) & p \in D(c, r) \\ 0 & p \notin D(c, r) \end{cases}$$

therefore it is C^∞ with respect to p.

For each point p on the surface, there is only finite number of hyperbolic disks covering it, therefore

$$f_i(p) = \frac{f_{D_i}(p)}{\sum_j f_{D_j}(p)}$$

is C^∞, so is the hyperbolic freeform surface $F(p) = \sum_i \mathbf{c}_i f_i(p)$.